

Modeling Contact Surface Edge Effects Using Boundary Elements

Thomas J. Curtin ⁽¹⁾, John M. W. Baynham ⁽²⁾, Robert A Adey ⁽²⁾

(1) Computational Mechanics Inc, 25 Bridge Street, Billerica, MA 01821

(2) Computational Mechanics BEASY, Ashurst Lodge, Southampton, Hampshire, SO40 7AA, UK

Contact details:

tcurtin@beasy.com

j.baynham@beasy.com

r.adey@beasy.com

ABSTRACT

This paper describes the application of the boundary element code BEASY as an analysis tool to investigate the acute variations in stress and displacement that occur at the edges of contacting surfaces. These “edge of contact” effects can be significant when frictional forces are present and play an important role when evaluating the susceptibility of a component to fretting fatigue damage. This point is substantiated by reports [1] from the U.S. Air Force (USAF) describing several disk post failures attributed to high stress gradients arising at the edge of contact between the blade and disk. Accurate representation of the stress and deformation at the edge of contact poses a difficult problem from the standpoint of computer modeling. Recent work using the finite element method [2] suggests that a very refined mesh in the area of contact is required to precisely capture the complex shear tractions and related stick-slip behavior. In addition to considerable mesh refinement at the edge of contact it is also important that the numerical technique used be able to simulate the progressive nature of the deformation. The Iterative-Fully Incremental contact solver used in the BEASY boundary element code uses a technique where the deformation and contact state are updated after each load increment providing a more realistic simulation of the loading and contact history. The accuracy of this boundary element code is validated against the well known Mindlin contact solution. The loading used in the validated computer model is modified slightly to simulate a typical fretting fatigue experiment. Two distinct load cases, distinguished by the magnitude of the applied bulk tensile stress, are used in these simulations. The shear traction and stick-slip behavior are predicted for discrete periods during the load cycle. This cycle consists of a maximum forward load, an unloading, a maximum reverse load, and a final unloading. The final section of this paper focuses on the analysis of a simplified dovetail joint; a common attachment feature in gas turbine engines. A parametric study is used to explore the sensitivity of contact stresses and stick-slip behavior to applied loading. There is discussion with regard to proper modeling strategy and solution time.

INTRODUCTION

The boundary element code BEASY is used to predict the “edge of contact” effects that occur when two surfaces with the same frictional properties are forced into contact. Because the traction and displacement gradients are high at the edge of contact, the modeling tool selected must be able to represent these acute variations. The basic formulation of a boundary element solution for non-conforming, frictional contact problems is introduced. A general overview of the Iterative-Incremental solution algorithm used in the numerical scheme is provided.

The boundary element method provides two significant advantages as a tool for solving contact mechanics type problems. Firstly, the primary variables of interest such as contact stress and relative tangential displacement are direct independent variables in the boundary element formulation. Secondly, the process of mesh refinement in the area of contact is simplified since only a surface mesh is required to model the two contacting bodies. Furthermore the mesh can be discontinuous enhancing the ability to grade the mesh toward the edges of contact. The locally refined mesh used in the area of contact must provide sufficient solution points in order to quantify the relatively small scale motion (fretting) that occurs between two surfaces in contact. This motion is oscillatory and varies, in both extent and magnitude, with the applied loading and frictional resistance.

Two different model geometries, both of which include non-conforming type surface contact, are solved to illustrate the ease of use and accuracy of the boundary element code. The first model represents a cylindrical body resting on a plane surface. The cylindrical body is loaded by a normal and tangential force and resisted by frictional forces at the contact interface. The predicted tractions are compared to those from the Mindlin contact solution. The load applied to the Mindlin contact model is then modified slightly by applying a bulk tensile stress to the plane surface. This modified load is similar to that typically used in fretting fatigue experiments. Computer simulations are used to illustrate the change in shear traction and stick-slip behavior that occurs during different phases of the loading.

The second model geometry represents a simplified dovetail joint. This type of attachment structure is routinely analyzed during the design of gas turbine engines. Given the fretting motions that commonly plagued such a connection it is susceptible to cracking that may be caused by contact related stresses. Cracks typically have been found at the trailing edge of contact ($x = -a$) where high tensile stress can occur, or just below the contact surface in areas of high shear stress. As a precursor to any type of fracture analysis it is imperative that accurate contact stresses be predicted.

A parametric study was performed using the dovetail joint model to determine the contact stress and stick-slip behavior for a range of applied loads. The effect of friction was

considered by analyzing models with ($\mu = 0.125, 0.25, \text{ and } 0.5$) and without friction ($\mu = 0$). The effect of frictional resistance to reduce the magnitude of the normal contact stress is significant. As such the frictionless case represents an “upper bound” on the value of the maximum normal contact stress.

BACKGROUND

The Engine Structural Integrity Program (ENSIP) was established by the U.S. Air Force to provide an organized and disciplined approach to the structural design, analysis, qualification, production, and life management of gas turbine engines [1]. As part of this mission it is important to predict accurate stresses and identify potential failure modes of critical structural components. The in-service material damage that may be produced by low cycle fatigue loading, fretting or fretting fatigue, and wear should be assessed [1].

These various modes of damage should be analyzed using sub-models containing the geometric details of the component, rather than larger, de-featured models of complete structural assemblies. The boundary element method is a useful structural modeling tool in this respect. Because of its mathematical formulation and surface only meshing capability, the boundary element method is well suited for predicting contact stress, and stress concentrations and gradients at structural discontinuities (i.e. bolt holes, rim slots and posts, radii, blade shrouds and dovetails).

Accurately determining the nature of contact stress is imperative to assess the durability of components subjected to fretting fatigue damage. An important component of the work described in this paper is the computer simulation of a fretting fatigue experiment. This simulation provides comprehensive information on the behavior of the fretted region including consideration of contact and friction stress interaction with applied mechanical stresses. This type of information is critical when making decisions regarding acceptable fatigue limits.

As aircraft approach or exceed their intended service lifetime issues of structural integrity reach paramount importance. Fretting fatigue cracking is a critical design concern for turbine engine blade disk attachments. Guidelines established by the USAF [1] state that in regions of contact, a crack, normal to the contact surface, should be assumed to develop during service. In order to properly analyze the impact of such a crack it is important to consider the bulk stress in the component in addition to contributions from the local stress field due to the contact loads. The USAF guideline suggests that there is need to perform coupled contact-fracture type problems. The boundary element method has the capability to perform coupled contact-fracture type analyses and could potentially serve as a comprehensive tool for investigating the effects of localized damage that are critical to making decisions regarding the HCF life of turbine engine components.

CONTACT MECHANICS USING BOUNDARY ELEMENTS

The boundary element method uses surface integral equations to analyze the behavior of bodies forced to come in contact. It is a mixed formulation method whereby both the tractions and displacements can be unknowns. As such these two variables are solved with the same degree of accuracy. The area of contact is not known a priori and thus the variables in the area of contact are formulated in such a way that they become part of the solution. The area of contact may contain regions of stick, slip, and separation. It is assumed that the frictional force acting along the slip region follows Coulomb's friction law.

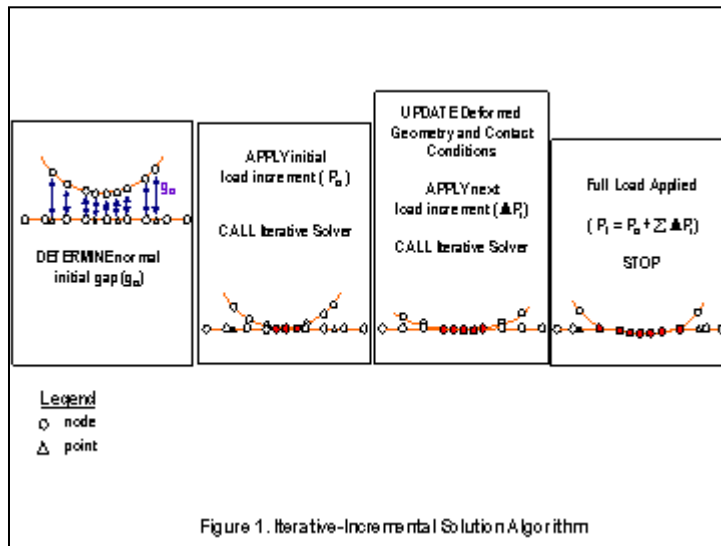
A numerical solution is obtained using a separate discretization for each contacting body. This produces two sets of linear equations that are expressed in matrix form. These two sets of equations share boundary variables in the contact region forcing the two sets of equations to be coupled. The two sets of equations are solved simultaneously for any combination of external load and contact condition. Direct solution of the contact stresses on the surface provides improved accuracy compared to other numerical techniques, particularly if the stress gradient with respect to depth below the contact surface is significant.

The non-conforming contact problem is both nonlinear and load path dependent. As such the extent of the contact region is determined as part of the solution using an iterative procedure to solve the coupled system of equations [3]. At each contact node, equations are formed to consider displacement compatibility and traction equilibrium. These compatibility and equilibrium equations are derived explicitly for each potential contact node by considering the contact state (separation, stick, slip). A unique solution technique is used whereby the entire system matrix does not need to be completely re-solved at each new iteration which significantly speeds up the solution process. This method is suitable for large-scale three-dimensional analysis and is numerically efficient.

Load Modeling Strategy

The BEASY boundary element code uses an Iterative-Incremental solution process (Figure 1). The first step in the process determines the initial separation of the surfaces by computing the normal gap distance between the two contacting surfaces. A small percentage of the full load is then applied to establish the initial contact conditions. A load scaling technique is used to ensure that the normal traction at the edge of contact is zero for the prescribed load increment (ΔP_i). The contact state for this intermediate contact configuration is determined and adjusted using an iterative technique that applies the necessary contact constraints to satisfy displacement compatibility and traction equilibrium. During this process checks are made for new nodes coming into contact, tension nodes are freed, and slip and stick modes are adjusted. In the case of a slip mode a special algorithm is used to ensure that the frictional force is set to oppose the relative displacement. After convergence is obtained in this iterative routine the deformed geometry and contact conditions are updated and the next load step is applied. This

process is repeated until the full load (ΔP_T) has been applied to the model and the final contact state determined.



This type of solution strategy where the deformed geometry and the contact status inside the contact region are updated through the use of previous boundary displacements and contact traction conditions after each load increment has the advantage of retaining both the contact history and the load history [4]. The Iterative-Incremental solution process also captures the phenomenon of Partial Slip (the progressive relative displacement between two bodies). Partial Slip is an important consideration in regions of advancing contact where a node in stick in the tangential direction for the current load increment may have undergone some slip during the previous load increment.

It is important that the load increments are not too large when modeling progressive contact problems in order to ensure an accurate contact history. If the size of the load increments is too large it is possible that sharp peaks in the tangential traction could result. This is often interpreted as being the results of a model that is “too stiff” [4] when the reality is that the contact history is not being accurately determined (i.e. missing periods of slip or partial slip).

MODELING THE MINDLIN PROBLEM

Mindlin Contact

The well known contact solution for two elastic cylinders pressed together by a normal force (P) and subsequently loaded by a shear force (Q) was derived by Mindlin [7]. If the radius of one of the cylinders is assumed to approach infinity the problem essentially reduces to a cylinder on a plane surface (Figure 2). The quantities of interest are the normal and shear tractions on the contact region. Equations describing the normal $p(x)$ and shear $q(x)$ components of the surface traction are reproduced below for completeness [8].

$$p(x) = p_o \sqrt{1 - \left(\frac{x}{a}\right)^2} \quad |x| \leq a \quad (1)$$

$$q(x) = -\mu p_o \sqrt{1 - \left(\frac{x}{a}\right)^2} \quad c < |x| \leq a \quad (2)$$

$$q(x) = -\mu p_o \sqrt{1 - \left(\frac{x}{a}\right)^2} + \mu p_o \frac{c}{a} \sqrt{1 - \left(\frac{x}{c}\right)^2} \quad |x| \leq c \quad (3)$$

where:

$p(x)$ = normal traction

$q(x)$ = shear traction

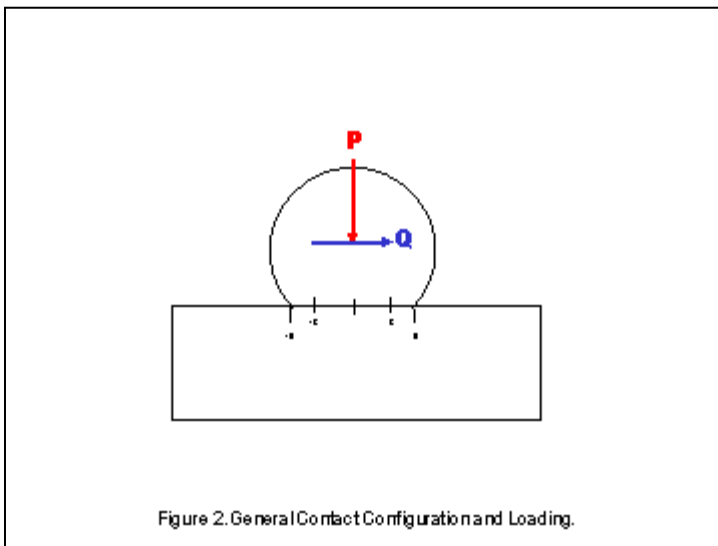
x = horizontal coordinate in contact model

c = stick zone half-width

a = contact half-width

μ = coefficient of friction

p_o = maximum normal traction under contact



Computer Model

A three-dimensional computer model representing a cylinder on a block was analyzed. The boundary element model and material properties are shown in Figure 3. Both the cylinder and block have the same material properties. Due to the symmetry of the problem, only half of the structure is modeled. The boundary mesh consists of 745 elements (10,974 DOF) with quadratic interpolation functions. The model includes multiple zones in order to apply boundary conditions and facilitate mesh refinement in the contact region (Figure 4).

The shear traction gradient is very high with a near singular behavior at the transition from stick to slip for this contact configuration and loading. As such the element sizes at these locations must be sufficiently small to accurately capture this behavior. Figure 5 shows the mesh used on the contact surface. There are total of 64 elements (329 nodes) on each prescribed contact surface. The mesh is biased in two directions relative to the centerline of contact with element edge lengths ranging from 0.002046 inch (51.9 microns) at the contact centerline to 0.0006821 inch (17.3 microns) near the anticipated edges of contact.

The loading and restraints used in the computer model are shown in Figure 6. The cylinder (Zones 4, 5) is restrained from rotation by a block (Zone 3) located above it that allows frictionless sliding along the common interface but prevents rigid body rotation of the cylinder. A distributed spring ($k_s = 18.3 \times 10^6$ psi) boundary condition is applied to the lower block (Zones 1, 2) to be consistent with elastic half-plane assumption in the Mindlin solution.

Loads are applied to the model using two separate Load Cases. Load Case 1 consists of a normal force $P = 1200$ lbs/in of axial length. Load Case 2 consists of both a normal force ($P = 1200$ lbs/in) and a tangential force of $Q = 270$ lbs/in of axial length. Load Case 1 is applied first to force the cylinder in contact with the plane surface and then Load Case 2 is used to introduce the horizontal force. It may appear that the normal force is applied twice, however Load Case 1 is actually removed simultaneously as Load Case 2 is applied so that the full load (P) is always maintained. This loading sequence is used to be consistent with the loading defined in the Mindlin problem.

Discussion of Results

The normal and shear tractions predicted by the computer model agree very well with the Mindlin solution. This agreement can be seen in the plots of normal and shear traction shown in Figure 7. It is encouraging to see that in addition to the maximum values being within approximately 1% of the Mindlin solution that the form of the tractions are also similar. The maximum shear traction occurs at the border of the stick-slip zone and is marked by two distinct peaks in value. The computer model predicts the magnitude of the peak shear traction reasonably well but there is a slight difference at the leading edge of contact ($x = a$). This difference can be attributed to the lack of an element node (or solution point) at this position. This highlights the need for a very refined mesh near the edge of contact particularly at the stick-slip transition zones.

A plot of the accumulated slip is shown in Figure 8. As expected the plot shows the slip profile to be symmetric relative to the centerline of the contact area. The maximum

accumulated slip occurs at the edge of contact and is 8.66×10^{-6} inch. The predicted contact half-width (a) and the stick half-width (c) are 0.01737 inch and 0.01285 inch respectively. These results are within less than 0.5% of the Mindlin values.

The contact stress and stick-slip behavior predicted by the computer model show excellent agreement with the Mindlin solution. It is important to note that an accurate solution was obtained without an excessive number of elements in the contact area. This leads to both reduced model building time and reasonable solution times. The three-dimensional computer model, including the geometry, mesh, restraints and loading was created in less than 1 hour and a converged solution obtained in 183 minutes.

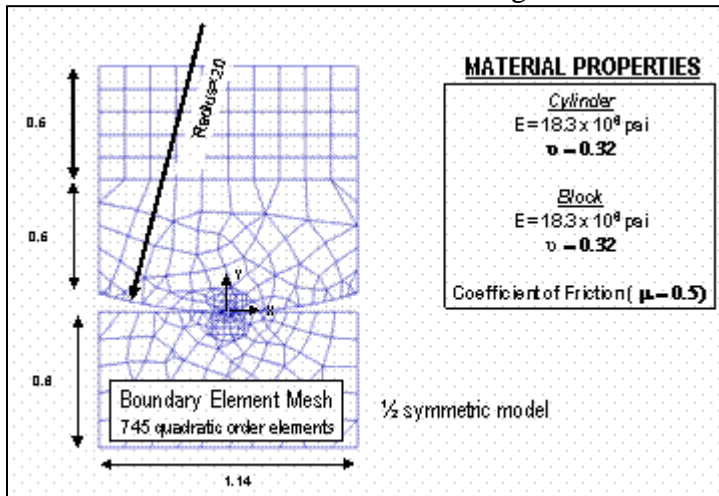


Figure 3. Boundary Element Model and Material Properties

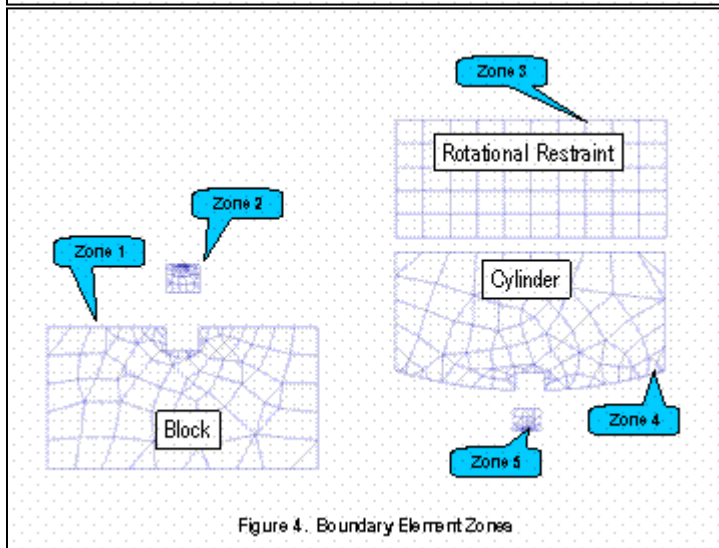
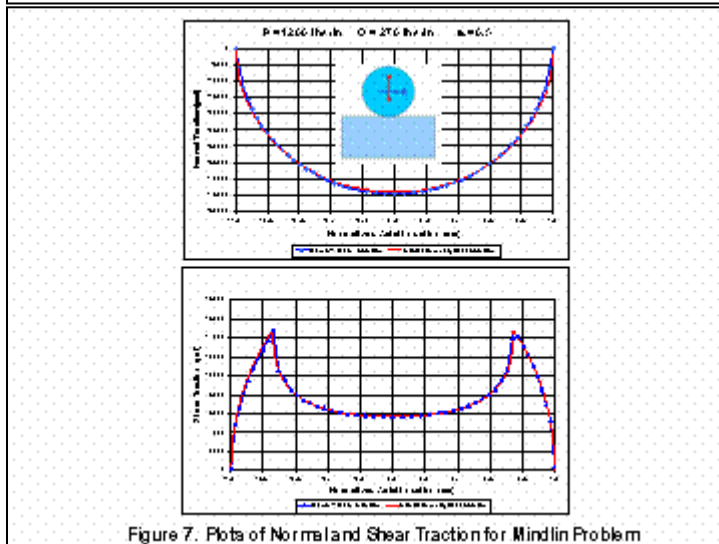
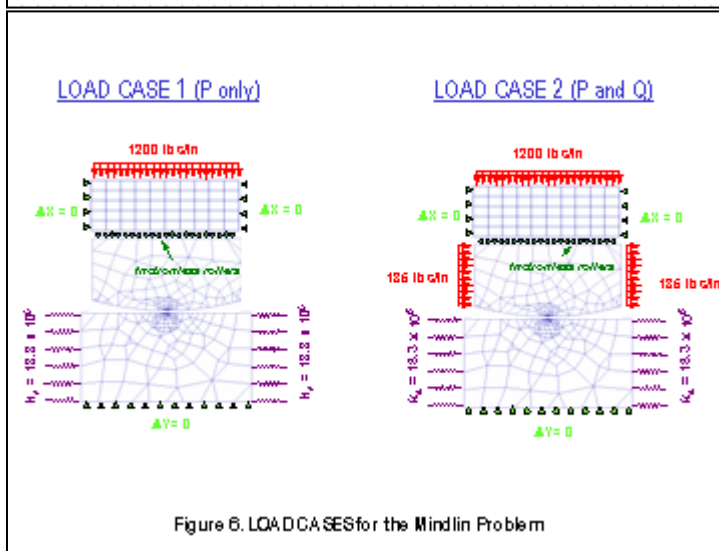
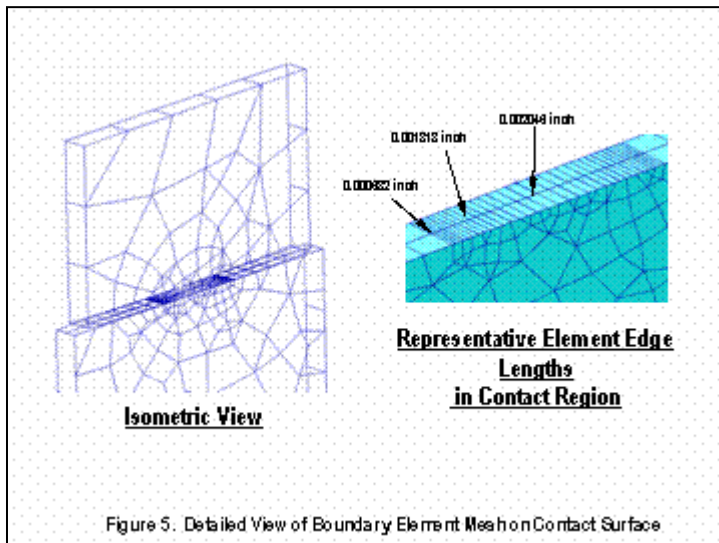
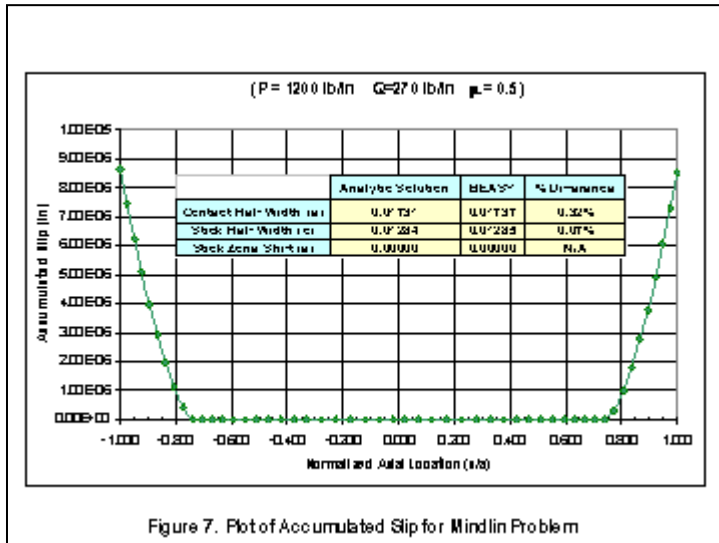


Figure 4. Boundary Element Zones



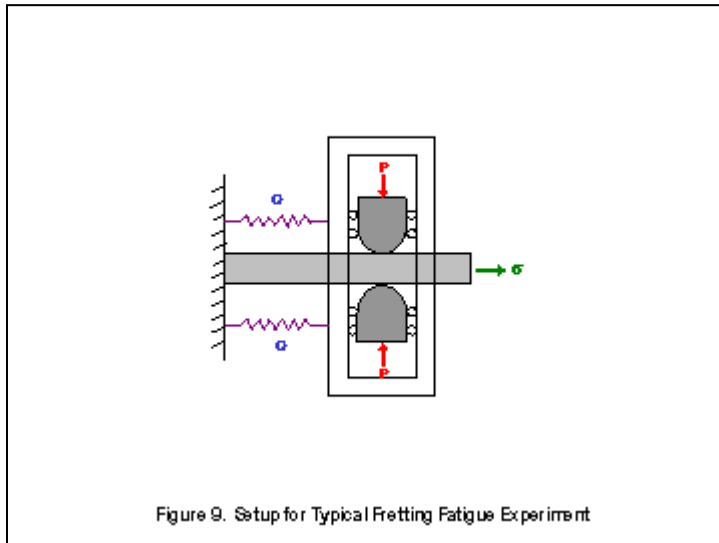


SIMULATING THE MECHANICS OF FRETTING

Fretting fatigue is an important concern in the design of parts subject to cyclical contact stresses such as blade disk assemblies, bearings, and other critical attachment structures. Figure 9 shows the configuration for one type of fretting fatigue experiment. This testing assembly is designed to apply a normal force through a cylindrical fretting pad to a test specimen. A bulk tensile stress is then applied to the specimen. Because the test specimen is restrained by fretting pads attached to stiff springs a simultaneous tangential force is generated at the contact interface.

The fretting problem is similar to the Mindlin problem discussed in the previous section with the exception of the application of a bulk tensile stress to the elastic half-plane. This tensile stress has a dramatic effect on the contact stresses and serves to modify the stick-slip zones when compared with the classic Mindlin solution. The nature of the shear traction is controlled by the magnitude of this applied tensile stress. The bulk tension either serves to shift the position of the stick zone or if it exceeds a critical value to introduce reverse slip at the leading edge of contact [8].

In general during a fretting fatigue test the tangential load (Q) and bulk stress (σ) are applied and relaxed in phase under a constant normal force (P). Assuming that Q and σ are increased simultaneously and proportionately from zero the surface shear traction will take one of two forms depending on the magnitude of the tensile stress [8].



Shifted Mindlin Case

The Shifted Mindlin Case, as the name implies, produces a shear traction similar to that described by Mindlin but with the center of the stick zone shifted a distance “ e ” toward the leading edge of contact. This case applies when the bulk tensile stress is small and the following inequality is satisfied.

$$\frac{\sigma}{\mu p_o} \leq 4 \left(1 - \sqrt{1 - \frac{Q}{\mu P}} \right) \quad (4)$$

The sign of the shear traction peaks are the same at both edges of the stick zone. The equations describing the form of the shear traction for this case are given below:

$$q(x) = -\mu p_o \sqrt{1 - \left(\frac{x}{a} \right)^2} \quad e + c < a \quad (5)$$

$$q(x) = -\mu p_o \sqrt{1 - \left(\frac{x}{a} \right)^2} + \frac{c}{a} \mu p_o \sqrt{1 - \left(\frac{x - e}{c} \right)^2} \quad |x - e| \leq c \quad (6)$$

where:

$e = x$ coordinate of the center of stick zone

Reverse Slip Case

The Reverse Slip case produces a shear traction that is defined by a peak value of opposite sign at the border of the stick-slip transition zone. This reversal in sign implies that a region of reverse slip occurs at the leading edge of contact. In addition to the sign reversal there is also a shift in the stick zone toward the leading edge of contact [8] that is caused by the tangential force (Q). The Reverse Slip case applies when the bulk tensile stress is large and when the following inequality is satisfied.

$$\frac{\sigma}{\mu p_o} > 4 \left(1 - \sqrt{1 - \frac{Q}{\mu P}} \right) \quad (5)$$

The full derivation of the shear traction solution for the Reverse Slip case can be found in the literature [8].

Computer Model

A simulation of the fretting fatigue experiment is accomplished with the same computer model used to represent the classic Mindlin problem. However the fretting simulation model includes the following modifications:

- 1) application of a bulk tensile stress (σ) to the block in contact
- 2) setup of Load Cases to simulate the phasing of Q and σ .

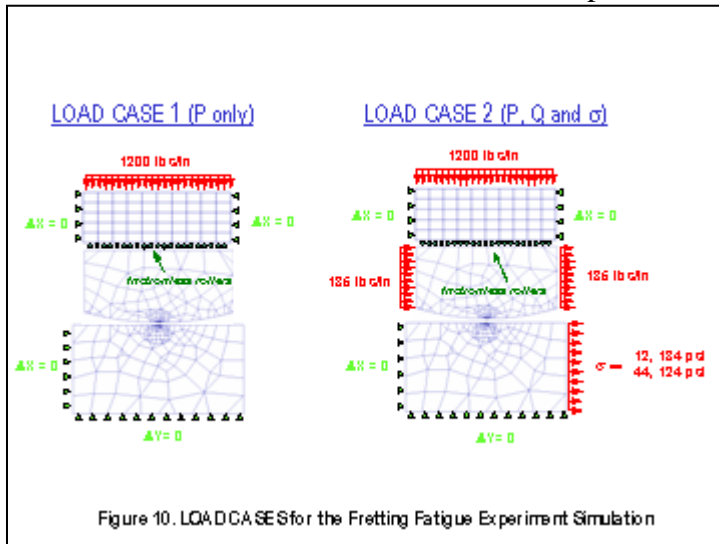
The loading used in a fretting fatigue experiment is cyclic in nature and includes a maximum forward load, an unloading, a maximum reverse load, and a final unloading. These four phases of loading are simulated in the boundary element model by sequencing appropriate Load Cases.

The Load Cases and required sequencing necessary to account for the loading and unloading phases are listed below (Figure 10).

- Load Case 1 – Vertical Load [P only]
- Load Case 2 - Maximum Forward Load [P, Q, σ]
- Load Case 3 - Unloading [P only, Q and σ reduced to zero]
- Load Case 4 - Reverse Loading [P, -Q, - σ]

Load Case 5 - Unloading [P only, -Q and $-\sigma$ reduced to zero]

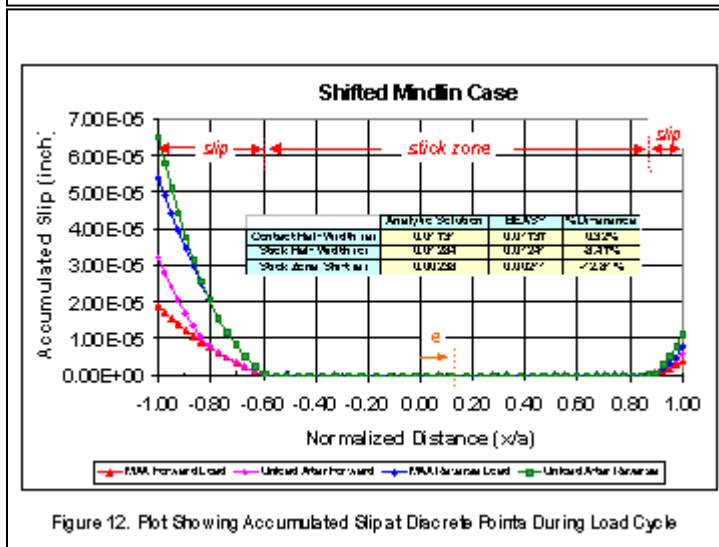
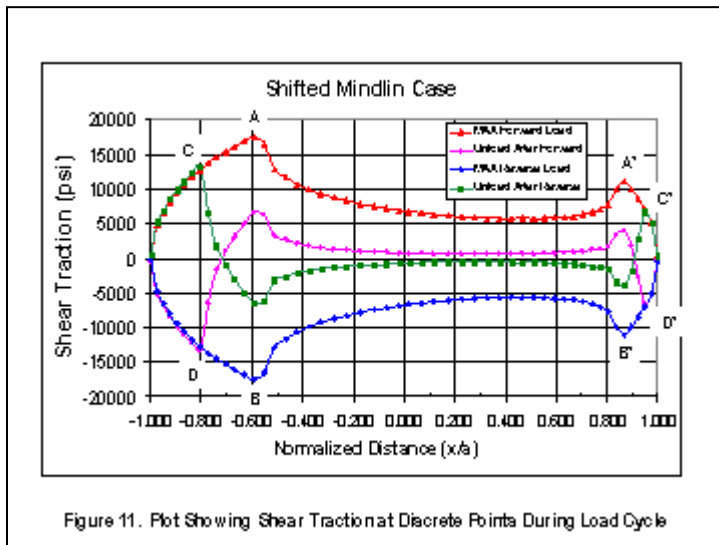
The shear tractions and stick-slip behavior for each phase of loading are predicted using two models. Each model has a unique value of the bulk tensile stress in order to simulate either the Shifted Mindlin case or Reverse Slip case.



Discussion of Results

The first simulation was performed using a bulk tensile stress of $\sigma = 12,134$ psi and is intended to represent the Shifted Mindlin case. This value of the bulk tensile stress in conjunction with the prescribed values of P, Q and μ satisfy the inequality described in equation (4). Shear traction and accumulated slip plots for the full loading cycle are shown in Figures 11 and 12 respectively. These plots show the shift in the center of the stick zone toward the leading edge of contact and the non-zero residual shear stress that remains after unloading. Approximately 25% of the peak shear traction remains at the trailing edge of contact after the unloading phase.

These plots also show that the borders of the stick zone are coincident with the peak shear tractions for both the forward and reverse loading phases (locations A, A' and C, C' on the plots). During both unloading phases there is some additional slip however the extent of this additional slip is controlled by the different position of the peak residual shear tractions (locations B, B' and D, D' on the plots). Effectively a limited region of no additional slip (or stick) is created. This region is bounded by the peak shear traction during the loading phase and the peak residual shear traction.



The second simulation was performed using a bulk tensile stress of $\sigma = 44,124$ psi and is intended to represent the Reverse Slip case. With the other loads being the same and this new value of the bulk tensile stress the inequality described in equation (5) is satisfied. The plots of predicted shear traction and accumulated slip obtained are shown in Figures 13 and 14 respectively. The presence of non-zero residual shear stress upon unloading and stick zone borders coincident with peak shear traction values is similar in nature to that found in the Shifted Mindlin case.

The main difference however is a reversal in the sign of the shear traction at the leading edge of contact and a much more extensive region of slip at the trailing edge of contact. The stick zone width for this case is about 70% less than that of the Shifted Mindlin case but the magnitude of shift in the stick zone is nearly double. Of particular interest is the fact that the stick zone width for the Reverse Slip case does vary with the magnitude of the bulk tensile stress unlike the Shifted Mindlin case [8].

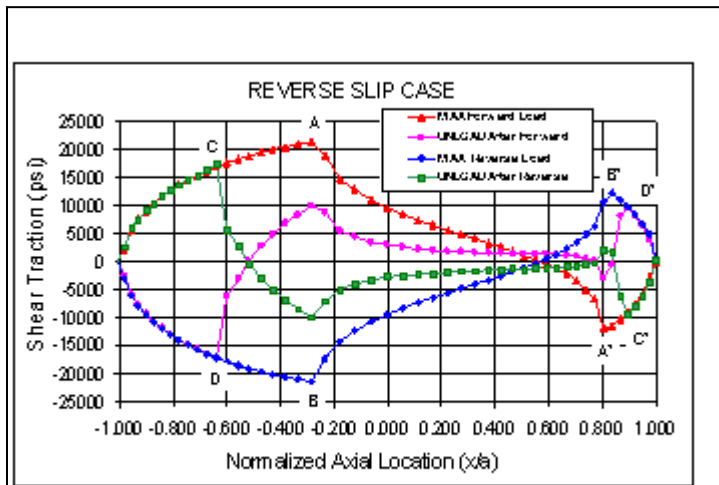


Figure 13. Plot Showing Shear Traction at Discrete Points During Load Cycle

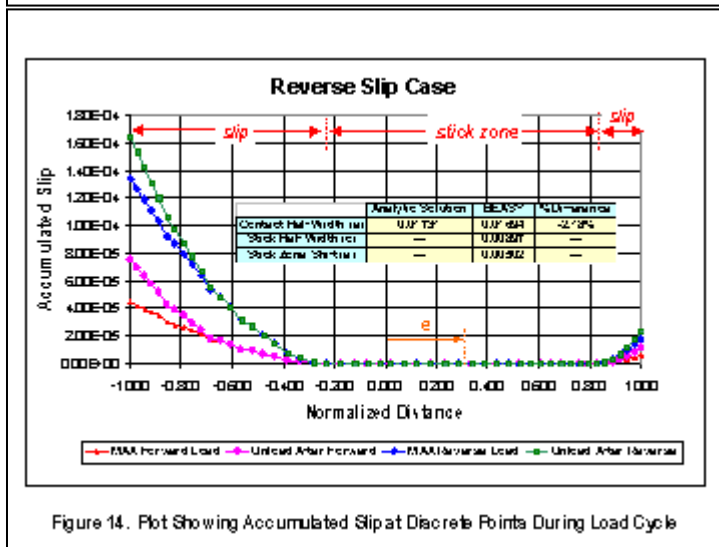
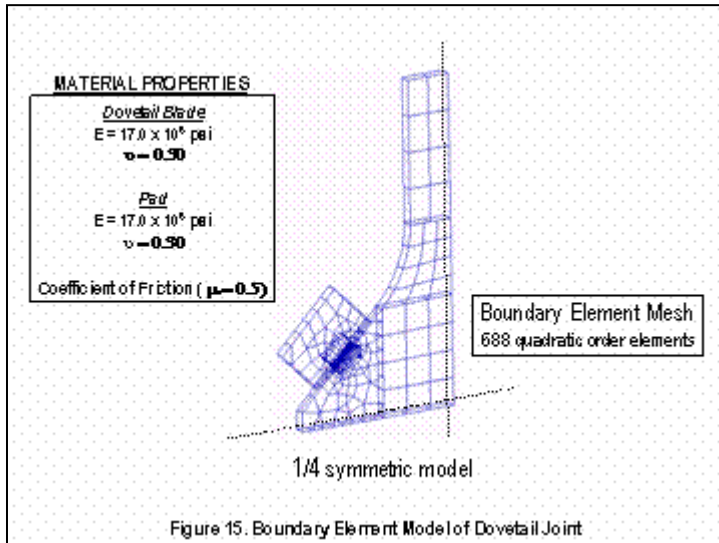


Figure 14. Plot Showing Accumulated Slip at Discrete Points During Load Cycle

These two computer simulations help explore the complex fretting behavior that occurs when frictional forces are present along the contact interface. Minimal effort was required to create the two fretting simulation models. Modification of one of the original Load Cases and setup of appropriate load sequencing was all that was required. Converged solutions were obtained in approximately 275 minutes for both cases.

DOVETAIL JOINT ANALYSIS

The final section of this paper discusses the boundary element modeling of a simple dovetail joint. The intent of this investigation is to simulate the mechanics of contact between a blade and rotor disk. The three-dimensional boundary element model and associated loading are shown in Figure 15. Both dovetail blade and pad were assumed to have the same material properties (elastic modulus $E = 17,000$ ksi; yield stress $\sigma_y = 130$ ksi; Poisson's ratio $\nu = 0.3$). The model was assumed to have a thickness of 0.1 inch. Because of symmetry only one-quarter of the structure is modeled.



Three computer models (Models A, B, and C), with different degrees of mesh refinement, were analyzed to check solution convergence. Table 1 shows the total number of elements, number of contact elements, contact element edge lengths, solution time, and maximum contact stress for each model. The model with the most refined mesh (Model C) has total of 686 elements with quadratic interpolation functions. Of the total number of elements, 172 were prescribed as contact elements with 92 on the surface of the dovetail and 80 on the surface of the pad. The contact element edge length on the dovetail is 0.00351 inch (89.2 microns). It should be noted that the meshes on the two opposing contact surfaces do not match. This is allowable from a modeling standpoint because of the node to surface contact solution used in the boundary element code.

Table 1

	Total # Elements	Total UCP	Number of Contact Elements	Minimum Element Edge Length on Dovetail (inch)	Minimum Element Edge Length on Pad (inch)	Solution Time (minutes)	MAX Normal Traction (ksi)	MAX Shear Traction (ksi)
Model A								
$\mu = 0.0$	363	4024	88	0.00774	0.00469	4	32.37	N/A
$\mu = 0.5$	363	4024	88	0.00774	0.00469	7	32.38	27.32
Model B								
$\mu = 0.0$	434	7434	172	0.00397	0.00253	23	33.24	N/A
$\mu = 0.5$	434	7434	172	0.00397	0.00253	43	33.73	27.33
Model C								
$\mu = 0.0$	686	10707	172	0.00351	0.00253	33	33.72	N/A
$\mu = 0.25$	686	10707	172	0.00351	0.00253	33	33.56	4.23
$\mu = 0.5$	686	10707	172	0.00351	0.00253	33	33.39	27.33
$\mu = 0.5$	686	10707	172	0.00351	0.00253	33	33.33	27.37

Notes:
 (1) Solution time (clock time) on a Pentium V17MHz single processor PC with 12 MB RAM
 (2) Results based on applied loading of 65.62 lbs

Discussion of Results

The data in Table 1 suggest that there was little difference in the maximum normal and shear tractions for the three models suggesting that the mesh refinement used in all three models was sufficient to accurately predict the stress and deformation fields. The data in Table 1 is based on an applied load of 65.62 lbs. Contact surface tractions for different

values of the coefficient of friction are shown for Model C and indicate that the frictionless case serves as an upper bound on the maximum normal contact stress.

A parametric study was performed using Model C and varying the applied load from 65.625 lbs to 262.5 lbs in three equal increments. The analysis was performed using a constant value ($\mu = 0.5$) for the coefficient of friction. The contact behavior predicted for the dovetail is significantly different than that observed for the fretting simulations. This appears reasonable given the different curvature of the two contacting surfaces and resultant loads acting at the contact interface. The shear traction does not have the characteristic high peaks that define the border of the stick-slip zone in the fretting models. Rather it has a smooth distribution with a single peak located at the approximate centerline of contact that corresponds with the point of maximum normal traction.

The variations in the normal and shear traction and the slip behavior between the dovetail blade and pad are shown in related plots of the data. Figure 16 shows the developing normal and shear tractions in the contact area and the corresponding increase in the width of the contact zone as the load is increased. The predicted stresses for this range of loading remain in the elastic range confirming that a linear elastic analysis is acceptable.

The maximum values of the normal and shear traction do not increase linearly with increased applied load confirming that the contact analysis is modeling a nonlinear phenomenon. There is also a slight shift in the location of the maximum normal and shear traction values toward the contact edge closest to the applied load. The plot of accumulated slip shown in Figure 17 also indicates that region of slip is biased slightly toward the contact edge closest to the applied load. It is possible that this shift is related to a slight rotation of the dovetail blade relative to the pad as the two bodies deform. In essence the center of contact may be moving in response to the bending moment component of load acting at the contact interface.

The plot of accumulated slip suggests that there is nearly complete sliding between the dovetail blade and pad. There appears to be a very small region of stick at the extreme edges of contact that doesn't seem to fully develop until the highest load is applied. The slip curve data in Figure 17 show that there is a small area in the vicinity of the maximum normal pressure where the slip remains constant. This area does not appear to change in extent with increasing load. It represents about 57% of the area of contact at low loads (65.60 lbs) and about 29% of the area of contact at the highest load (262.50 lbs). The slip gradually declines from this area in both directions toward the edges of contact.

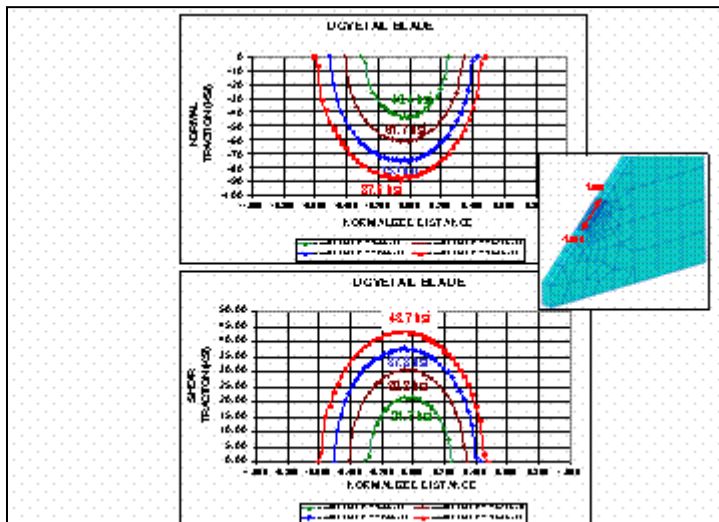


Figure 16. Plots of Normal and Shear Traction for Dovetail Joint

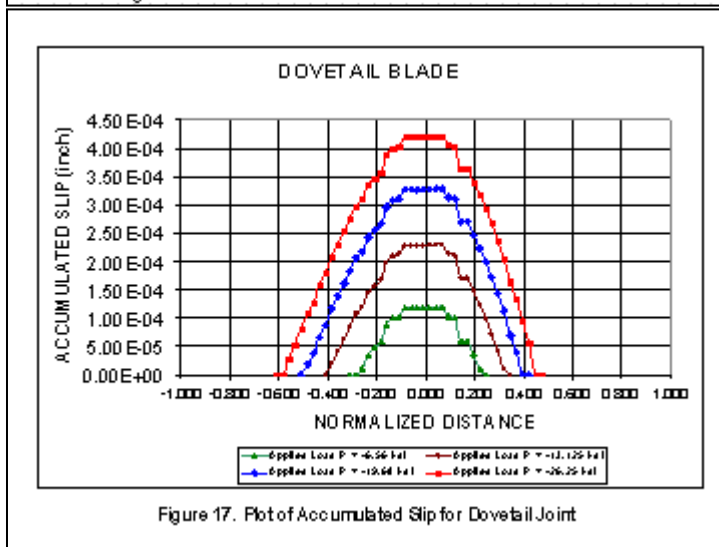
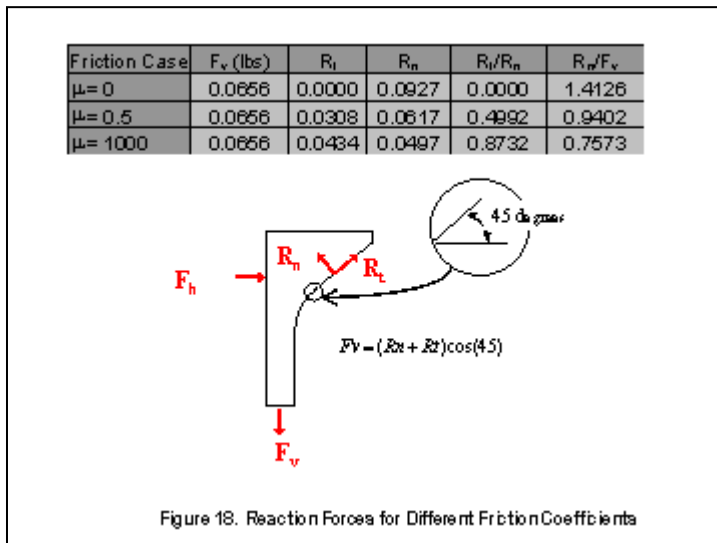


Figure 17. Plot of Accumulated Slip for Dovetail Joint

The cyclic behavior that may lead to this fretting fatigue cracking was also evaluated by unloading the model in various stages. An example of this is shown using the shear traction plot (Figure 18). For this example the load is increased from 196.8 lbs to 262.50 lbs and then unloaded back to 196.8 lbs. This loading/unloading sequence results in a slightly different shear traction at the 196.8 lbs level. The magnitude of the shear traction is reduced by approximately 5% and is characterized by two sharp peaks of reversed sign near the edge of contact.



SUMMARY

Simulating the mechanics of contact between two bodies is a complex and inherently non-linear problem because of the frictional forces on the contact interface and due to the fact that the size of the contact zone varies with applied load. Although analytical contact solutions are useful to validate numerical techniques they are limited in scope of application. The complex geometry typical of real engineering problems along with the nonlinear nature of the contact suggests that numerical methods are the only feasible means of obtaining precise solutions. The results presented in this paper demonstrate that the boundary element method is an accurate and economically feasible tool for solving non-conforming, frictional contact problems. The mathematical formulation of the boundary element method provides direct solution of the surface tractions in the area of contact. The Iterative-Incremental Contact Solver captures the progressive nature of the deformation between the contacting bodies and accurately models the impact of frictional forces on the stress field in the region of contact.

The BEASY boundary element code was first validated against the Mindlin contact solution, and then used to simulate the mechanics of fretting and analyze a dovetail joint; a common attachment feature in gas turbine engines. The normal and shear tractions and relative tangential slip at the contact interface are predicted with a high degree of accuracy for all three cases. These results were achieved without significant modeling effort and the solution times were reasonable for a frictional type contact problem.

Frictional forces play an important role when trying to understand their impact on the stress field and the stick-slip behavior between contacting bodies. The work in this paper shows that considerable peaks in shear traction can occur at the edge of stick-slip zones and that significant residual shear tractions can remain after unloading. This was observed in both the fretting simulation models and in the dovetail model. When friction is introduced into the analysis it also has an impact on the normal traction. In order to accurately predict the normal traction it is imperative that the development of frictional

forces that contribute to the development of the shear tractions be simulated with a high degree of precision.

This modification in the stress field due to friction is of great concern from the perspective of fretting fatigue cracking. An accurate contact analysis serves to better locate potential sites of crack initiation and thus provides useful information for determining inspection routines as well as providing the basis to perform more advanced fracture mechanics analyses required as part of damage tolerance design programs.

REFERENCES

- [1] MIL-HDBK-1738 B Feb 15 ,2002
- [2] Calcaterra, J. and Farris, T.N., “Analysis of Turbine Engine Attachment Fatigue Using Integral Equation Methods”, ICAF 2002,
- [3] Martin, D. and Aliabadi, M.H., “Boundary Element Analysis of Two Dimensional Elastoplastic Contact Problems” Eng. Analysis with Bound. Elements, Vol 21 pp 349-360, 1998
- [4] Man, K.W. Contact Mechanics using Boundary Elements, WIT Press, 1994, Topics in Engineering Vol. 2.
- [5] Johnson, K.L., Contact Mechanics, Cambridge University press, 1985
- [6] Boresi, A.P. et. al , Advanced Mechanics of Materials, 1993, John Wiley and Sons
- [7] Mindlin, R.D., Compliance of Elastic Bodies in Contact, J. Appl. Mech, 16, 259-268, 1949
- [8] Nowell, D. and Hills, D.A., “Mechanics of Fretting Fatigue Test” *Int. J. Mech Sci.* Vol 29, (1987), pp 355-365.
- [9] Zen, R. and Glodez S., “Service-Life Estimation of Contacting Mechanical Elements in Regard to Pitting”, Computational Mechanics, Techniques, and Developments, CIVIL-COMP Ltd., (2000), pp 203-209
- [10] Szolwinski, M.P. and Farris, T.N., “Mechanics of Fretting Fatigue Crack Formation”, Vol. 198, (1996), pp 93-107.
- [11] McVeigh, P.A., Harish, G., Farris, T.N. and Szolwinski, M.P., “Modeling Contact Conditions in Nominally-Flat Contacts for Application to Fretting Fatigue of Turbine Engine Components,” *International Journal of Fatigue*, 21 pp S157-165 (1999)
- [12] Johnson, K.L., “The Strength of Surfaces in Rolling Contact”, Proceedings of the Institution of Mechanical Engineers, 203, pp. 151-163, 1989.
- [13] Bentall, R.H. and Johnson, K.L., “Slip in the Rolling Contact of Two Dissimilar Elastic Rollers”, *Int. Journ. Mech Science*, Vol. 9 pp384-404, (1967)
- [15] Ghaderi-Panah A. and Fenner R.T., “ A general boundary element method approach to the solution of three-dimensional frictionless contact problems. Eng. Analysis with Bound. Elements, Vol 21 pp 305-316 1998